Piezoresistive graphite/polyimide thin films for micromachining applications

A. Bruno Frazier and Mark G. Allen
School of Electrical Engineering, Microelectronics Research Center, Georgia Institute of Technology, Atlanta, Georgia 30332-0250

(Received 30 July 1992; accepted for publication 4 January 1993)

In this work, graphite/polyimide composite thin films are introduced and characterized for micromachining applications. The material consists of submicron-sized graphite particles suspended in a benzophenone tetracarboxylic dianhydride–oxydianiline/metaphenylene diamine polyimide matrix. The resultant material represents a low cost, plasma-definable polyimide material which has been found to have a large piezoresistive coefficient over a range of graphite loadings. Selected film properties: Young's modulus, residual stress, and piezoresistivity are investigated for a graphite loading range of 15%–25% by weight using a slightly modified *in situ* load/deflection technique. Results of mechanical property characterization show that the residual stress is independent of graphite loading and the Young's modulus increases with increasing graphite loading. The maximum piezoresistive coefficient (gage factor) is 16.8 and occurs at a graphite loading of 18%.

INTRODUCTION

The advantages of polyimide films for use in microelectronics related applications have been well-documented. Polyimides have proven useful in hybrid microelectronic technology as both an interconnect and multichip module material due to their superior insulating properties and low relative permittivity. Polyimides are also used extensively as a planarization material in the fabrication of integrated circuits. The focus of our work is to investigate conductor-filled polyimides as potential materials for low-cost piezoresistive micromachined structures.

Consider the case of a large number of conductor particles suspended in a compliant film. When the film is strained (either in tension or compression), the number of particles in contact with each other (or the effective resistance between particles) will change. Thus, the overall resistance of the film will increase or decrease if the film is loaded in compression or tension. This piezoresistive effect could then be exploited for microsensor applications. The major advantage of such a piezoresistive material is that it can be spin-cast or screen printed onto a variety of substrates, resulting in a low-cost, piezoresistive material.

Conductive metal-filled polyimides have been widely studied for use in a variety of applications including die attach, thermistors, electromagnetic shielding, antistatic devices, pressure, and chemical sensors as well as aerospace applications where both a cost and weight savings can be realized over conventional metallic components. A large number of conductive fillers have been characterized for these applications including predominantly metallic fillers such as salts of silver, gold, palladium, cobalt, lanthanide, and copper (e.g., Refs. 1–6). Although these conductive materials exhibited interesting and useful characteristics, the majority were not compatible with conventional methods of microelectronics processing (e.g., plasma etching for pattern definition) needed for micromachined device fabrication. Studies have also been performed on characterizing organic fillers including graphite, but for applications other than micromachined systems.

In this work, graphite/polyimide thin film composites are prepared and characterized for microsensor system applications. The characteristics of interest include the piezoresistive coefficient (or gage factor) as well as the general mechanical properties of the thin film, residual stress and Young's modulus. Many techniques have been demonstrated for measuring the mechanical properties of thin films. These techniques include the common substrate curvature technique as well as many others which utilize micromachining technology. Those utilizing micromachining techniques and devices include stationary and movable structures,[7–12] and load/deflection testing of cantilever beams[13–15] and membranes.[16–19] Load/deflection of membranes has the following advantages: simultaneous measurement of the residual stress and the Young's modulus; being independent of the index of refraction of the material (useful for a composite); and being relatively insensitive to the surface roughness (also useful for a composite). In the following sections, the desired material properties are determined using an *in situ* membrane load/deflection technique involving simultaneous measurement of load, deflection, and resistance. The material properties of the composite films are evaluated for a graphite loading range of 15%–25%.

EXPERIMENTAL

The graphite/polyimide material is composed of submicron graphite particles obtained from Johnson Matthey Electronics and DuPont PI-2555 polymide (a benzophenone tetracarboxylic dianhydride–oxydianiline/metaphenylene diamine formulation). The composite is formed by introducing various quantities (loadings) of the graphite particles into the as-received PI-2555 polyamic acid solution in N-methylpyrollidone (NMP). The materials are mixed using a ball mill rotating at 4–5 rpm. The

 0021-8979/93/094428-06$06.00

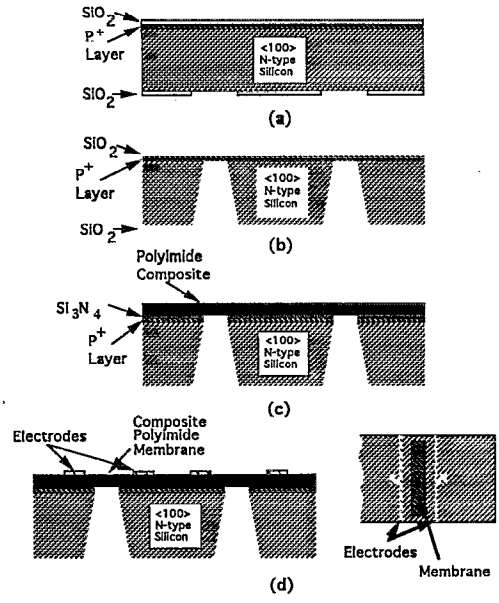

FIG. 1. Fabrication process for the rectangular membranes of composite material. The membranes are used to determine the material characteristics by load/deflection techniques.

mixing period is held for at least 72 h in order to insure homogeneity of the mixed composite solution. The composition of the films is based upon the weight percentages of the two constituents in the fully cured film. The weight of the polyimide in the cured film is calculated using the average percent solids of the polyimide solution.

To characterize the composite material, load/deflection testing[16,17] is performed using long rectangular membranes of the thin films which are fabricated on silicon substrates. The suspended membranes of the graphite-filled polyimide are realized using micromachining techniques. In the fabrication process, 2 in. ⟨100⟩ silicon wafers are anisotropically etched from the unpolished side in a 20 wt % potassium hydroxide solution heated to 56 °C (etch rate ~ 16 μm/h in the ⟨100⟩ direction).[20] The etching process, which takes ~ 18 h, uses a thermally grown 5000 Å silicon dioxide layer as an etching mask for both sides of the wafer. Long rectangular windows are patterned in the SiO_2 on the unpolished side of the wafer using a buffered oxide etchant. A 3–5 μm thick, heavily boron doped ($> 10^{20}/cm^3$) layer is used as an etch stop layer[16] on the polished side to produce a silicon membrane, Figs. 1(a) and 1(b). After the silicon etch is complete the silicon dioxide is removed, followed by deposition of an insulating layer of plasma-enhanced chemical vapor deposition (PECVD) Si_3N_4. The Si_3N_4 isolates the overlying composite material from the underlying heavily doped p^+ boron region. A thin film of composite material is applied over the Si_3N_4 using a multicoat procedure, Fig. 1(c). A single coat of the multicoat procedure consists of a 3000 rpm, 60 s spin cycle followed by a 15 min soft bake at 150 °C. The multicoat film is then fully cured at 400 °C for 1.0 h in a conventional oven. The p^+ etch stop layer and Si_3N_4 thin films are removed from the membrane regions by exposing

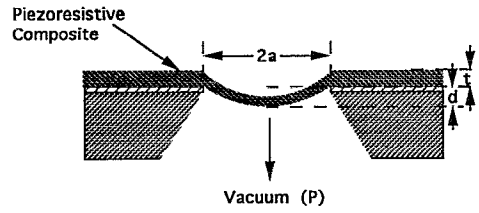

FIG. 2. A membrane of thickness t and width $2a$ undergoing a deflection d in response to a uniform applied load P.

the unpolished side of the wafer to a 95% CF_4/5% O_2 plasma, resulting in the finished composite membrane. At this point, the mechanical properties (Young's modulus and residual stress) can be determined from the load/deflection behavior of the membrane.

In order to determine the piezoresistive coefficient or gage factor, the fabrication process for the membranes must be extended to patterning the film and depositing electrodes for resistance measurements concurrently with the load-deflection measurements. The film is patterned into a 32 mm long strip using a 100% O_2 plasma and sputtered aluminum as the etch mask. The electrodes are then patterned in the aluminum etch mask as the final step in the membrane fabrication process, Fig. 1(d).

The characterization of the thin films is carried out using a material characterization station which allows application and simultaneous measurement of the pressure load to the membrane. The station operates by using dual vacuum lines. A constant vacuum is used to seal the membrane sample to the surface of the test apparatus. A second, controllable vacuum acts as the load to the membrane region. A pressure transducer is used to monitor the amount of the load induced by the second vacuum. The induced deflection at the center of the membrane is measured using a z-axis digimatic indicator mounted on the microscope to measure the microscope head travel necessary to keep the deflecting membrane in focus. As the membrane is deflected, the resistance is monitored by attaching probes to the electrodes patterned on the composite material.

MECHANICAL PROPERTIES

In this work, the mechanical characteristics are determined by an analysis of the load/deflection behavior of a membrane using an energy minimization approach,[21] but modified to account for the presence of residual tensile stress[16] and rectangular dimensions.[17] Consider the membrane shown in Fig. 2 deflecting under the application of a uniform pressure P. If the membrane is long compared to its width, it can be shown that the relationship between the applied pressure and center deflection of the membrane is given by

$$\frac{Pa^2}{dt}=2\sigma_0+\frac{4E}{3(1-\nu^2)}\left(\frac{d}{a}\right)^2, \tag{1}$$

where P is the applied pressure, E is the Young's modulus of the film, σ_0 is the residual stress in the film, ν is Poisson's

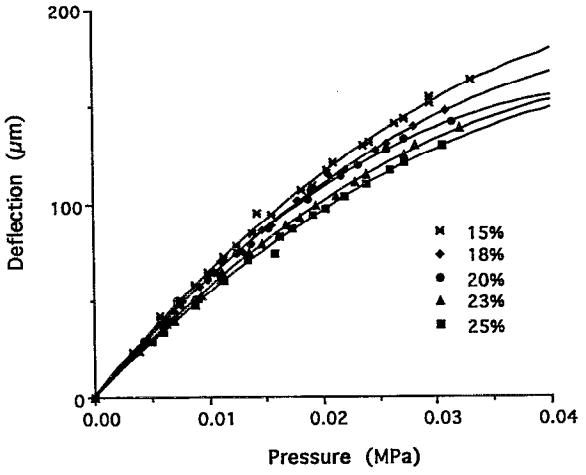

FIG. 3. Typical load/deflection characteristics for the graphite/polyimide composite material. The membrane was 30 mm long, 5 mm wide, and had a thickness range of 12–15 μm.

ratio of the film, $2a$ is the membrane width, t is the film thickness, and d is the membrane deflection at its center. Examination of Eq. (1) shows that if pressure–deflection data are plotted with (Pa^2/dt) on the y axis and $(d/a)^2$ on the x axis, the data should fall on a straight line. The residual stress can then be determined from the y intercept of the line and the plane strain modulus, $E/(1-\nu^2)$, can be determined from the slope of the line.

Typical load/deflection data are shown in Fig. 3. The data are for membranes of width $2a=4.76$ mm, length of 27.7 mm, and thicknesses ranging from 12 to 14 μm, depending on the graphite loading. Load/deflection tests were performed at 26 °C with a relative humidity of 35%. The mechanical characteristics are obtained by fitting the data to Eq. (1), as shown in Fig. 4. The scatter at low values of deflection in Fig. 4 is due to the difficulty in measuring small deflections using our material characterization station.

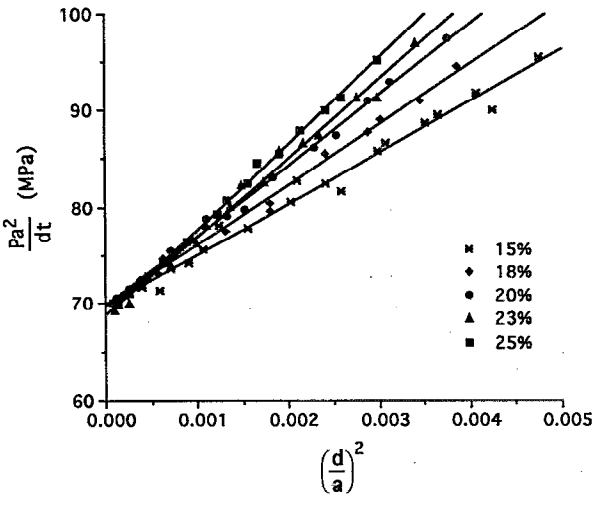

FIG. 4. Load/deflection data plotted in accordance with Eq. (1) for the graphite/polyimide composite films. The residual stress can be determined from the y intercept and the plane strain modulus from the slope.

TABLE I. Experimentally determined residual stress and Young's modulus for the composite material. The graphite loading range of the composite is 15%–25%.

% graphite	Residual stress (MPa)	Plane strain modulus (GPa)	Young's modulus (GPa)[a]
15	35.0±0.2	4.1±0.4	3.4±0.3
18	35.2±0.4	4.9±0.3	4.1±0.2
20	33.9±0.3	5.4±0.4	4.5±0.3
23	34.6±1.2	6.3±0.6	5.3±0.5
25	34.9±0.7	6.7±0.4	5.6±0.3

[a]Assumed $\nu=0.40$.

The experimentally determined residual stress and plane strain modulus, $E/(1-\nu^2)$, for a variety of film loadings are shown in Table I. The data represent the average of three membranes from each graphite loading percentage with the error given as the standard deviation of the three samples. In order to extract the Young's modulus, E, the experimentally determined plane strain modulus along with an average Poisson's ratio of 0.4 (Refs. 22 and 23) is used. As can be seen in Table I, the residual stress of the thin film is not significantly affected by the percentage of graphite loading for the range of 15%–25%. This result indicates that the organic portion of the composite dominates the residual stress characteristic. However, the plane strain modulus of the films does show a dependence on the amount of graphite loading. As the amount of graphite increases in the composite, the plane strain modulus of the material also increases. This result is expected based on the fact that the graphite particles characteristically have a much higher Young's modulus than the polymer.

PIEZORESISTIVE COEFFICIENT

The piezoresistive characteristics are determined by similar load/deflection techniques in which the resistance across the membrane is monitored as a function of deflection. Using the experimentally determined resistance/deflection relationship coupled with the model presented below, the piezoresistive coefficient (gage factor) can be obtained. It is assumed that the resistivity of the composite material has the form

$$\rho=\rho_0(1+\lambda\epsilon), \tag{2}$$

where ρ_0 is the resistivity of the unstrained composite material, λ is a dimensionless piezoresistive coefficient (gage factor), and ϵ is the strain induced by the deflection.

In order to find the resistivity and gage factor, the membrane is modeled by a combination of variable and constant resistors. Referring to Fig. 5, the resistance R_c represents the constant series resistance of the unstrained material in the regions c_1 and c_2 and can be expressed as:

$$R_c=\frac{\rho_0 c}{Lt}, \tag{3}$$

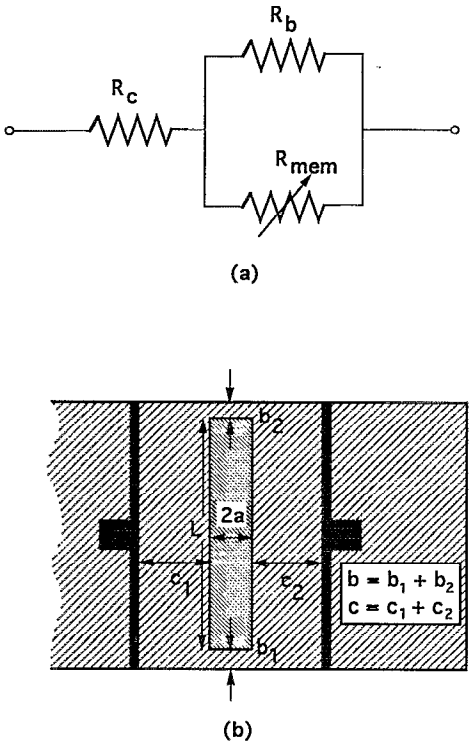

FIG. 5. (a) Equivalent resistive circuit of the membrane structure. (b) Schematic top view of a micromachined composite membrane structure. The relevant dimensions for modeling the resistance as a function deflection are shown.

where $c=c_1+c_2$, is the total series length of material which remains unstrained between the two electrodes, L is the membrane length, and t is the film thickness. In addition, there is a constant parallel "leakage" around the edges of the membrane which can be expressed as:

$$R_b=\frac{\rho_0 2a}{bt}, \tag{4}$$

where $b=b_1+b_2$ is the total parallel width of material which remains unstrained between the two electrodes, $2a$ is the membrane width, and t is the film thickness. The variable deflecting membrane resistance R_{mem} can be expressed as:

$$R_{\text{mem}}=\frac{\rho_0(1+\lambda\epsilon)2a}{Lt} \tag{5}$$

by combination of the standard resistance formula with Eq. (2).

In order to relate Eq. (5) to measured data, a relationship between the average membrane strain and the deflection at the center of the membrane must be determined. Assuming that the center deflections are small compared with the width of the membrane, the strain can be approximated as:[21]

$$\epsilon=\frac{1}{2}\left(\frac{dw}{dx}\right)^2, \tag{6}$$

where $w(x)$ is the shape of the deflected membrane and can be approximated as:[21]

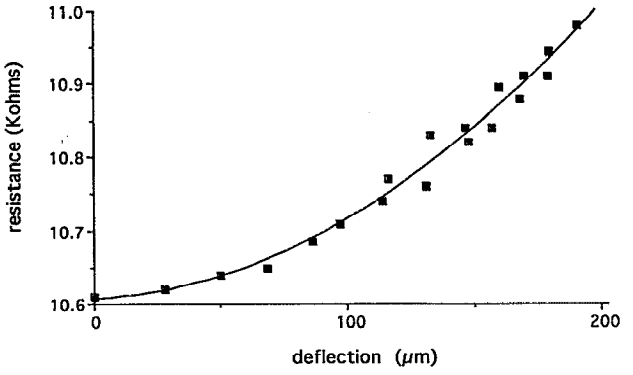

FIG. 6. Typical experimental data for the resistance change when applying a load to the membrane.

$$w(x)=d\left[1-\left(\frac{x}{a}\right)^2\right]. \tag{7}$$

Substitution of Eq. (7) into Eq. (6), taking the integral average over the membrane width, $(-a\leqslant x\leqslant a)$, substituting the result into Eq. (5), and combining the three resistors yields the relationship between total resistance between the electrodes and the membrane center deflection

$$R(d)=\rho_0\left(\frac{\alpha_1+\alpha_2\lambda d^2}{\alpha_3+\alpha_4\lambda d^2}\right), \tag{8}$$

where

$$\alpha_1=(2a+c)^2,$$

$$\alpha_2=4(2a+c)/3a,$$

$$\alpha_3=t(2a+c)(L+b),$$

$$\alpha_4=4bt/3a.$$

Note that all of the alpha coefficients as defined in Eq. (8) and Fig. 5 are known. Using this model for $R(d)$, it can be seen that a plot of $[-\alpha_1\rho_0+\alpha_3R(d)]$ versus $\{[\alpha_2\rho_0-\alpha_4R(d)]d^2\}$ should be linear and pass through the origin. The piezoresistive coefficient (λ) can then be determined from the slope of this line. It should be noted that under the case of zero deflection, Eq. (8) reduces to that expected for the unstrained membrane

$$R(0)=\frac{\rho_0(c+2a)}{t(L+b)}. \tag{9}$$

Measurement of the piezoresistive coefficient (λ) is performed as follows. First, an unstrained resistance measurement is taken and the unstrained resistivity ρ_0 is determined from Eq. (9). Then, a resistance measurement as a function of deflection is taken. These results are plotted in accordance with Eq. (8) as described above. Finally, the piezoresistive coefficient is determined by the slope of this plot.

A typical resistance/deflection curve is shown in Fig. 6. For this sample, the membrane width $2a$ was 4.76 mm, the film thickness was 12.5 μm, the graphite loading was 18 wt %, and the parameters b and c were 4.56 and 3.7

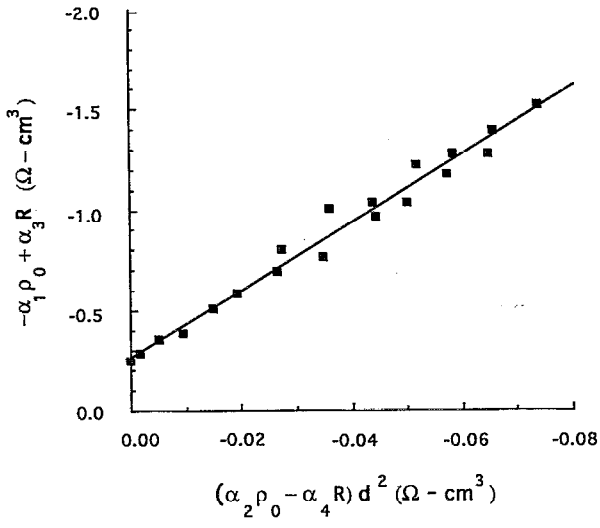

FIG. 7. Resistance–deflection data of a graphite/polyimide composite film with 18% graphite loading plotted in accordance with Eq. (8). The piezoresistive gage factor is determined to be 16.8.

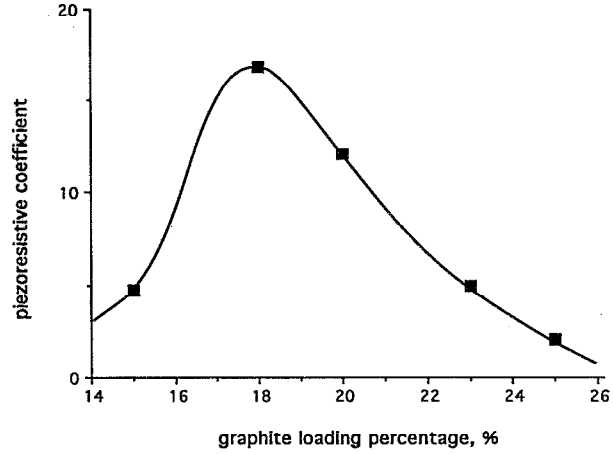

FIG. 9. Piezoresistive gage factor of the graphite/polyimide composite material as a function of graphite loading. The maximum piezoresistive coefficient is obtained for a loading of 18% graphite and tails off for loading percentages above and below the 18% value.

mm, respectively. The data plotted in accordance with Eq. (8) is shown in Fig. 7. The data fall on a straight-line, indicating that Eq. (8) is obeyed. From this plot, a value for the piezoresistive coefficient (gage factor) of 16.8 was determined.

The results obtained for the unstrained resistivity (ρ_0) and the piezoresistive coefficient (λ) of the composite film over a graphite loading range of 15%–25% are shown in Figs. 8 and 9, respectively. As can be seen, the maximum piezoresistive coefficient is obtained for a graphite loading of 18%. The obtained piezoresistive coefficients are quite large. For example, selecting a typical strain of 1% in a composite thin film with 18% graphite loading will induce a 16.8% change in total resistivity. The experimentally determined values are comparable to those obtained for doped polysilicon thin films.[24]

The piezoresistive coefficient tails off for loading percentages above and below the optimum value as the material becomes increasingly insulating or conductive. This can once again be correlated to the change in proximity of neighboring conductive particles. In loading percentages below the optimum value, the proximity of neighboring conductive particles becomes increasingly larger, therefore, the change in proximity as a result of induced strain on the material is small resulting in small changes in the resistivity of the film. For loading percentages greater than the optimum value, the number of nearest neighbors increases to the point where the proximity is uneffected by the strain on the material.

In addition to characterizing the piezoresistivity of the material, another interesting characteristic of the composite graphite/polyimide material has been investigated, the dependence of resistivity on temperature. The characterization test consisted of monitoring the unstrained resistivity, ρ_0, of the material over a temperature range of 25–150 °C at a constant relative humidity level of 35%. Tests were performed on multiple membranes for each graphite loading percentage. Multiple temperature cycles were performed on each membrane with consistent results. Figure 10 shows typical data of ρ_0 plotted versus T^{-1} for 18%

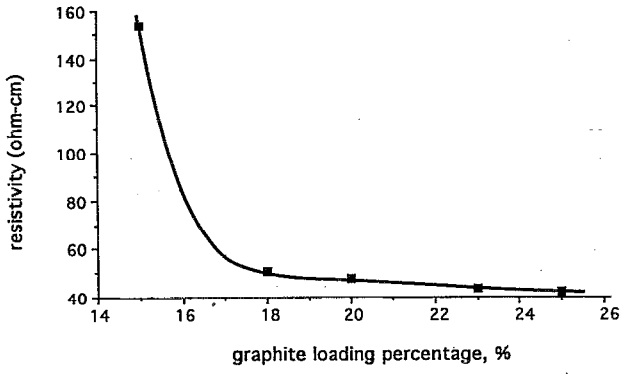

FIG. 8. Experimentally determined average resistivities (ρ_0) for graphite/polyimide thin films for a loading range of 15%–25%.

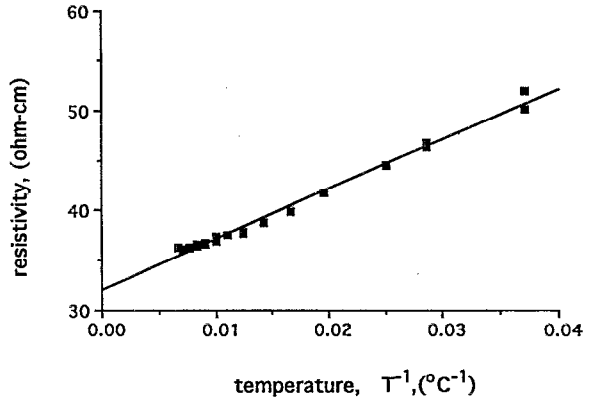

FIG. 10. Typical dependence of the unstrained resistivity, ρ_0, on the ambient temperature. The data are for an 18% graphite loading.

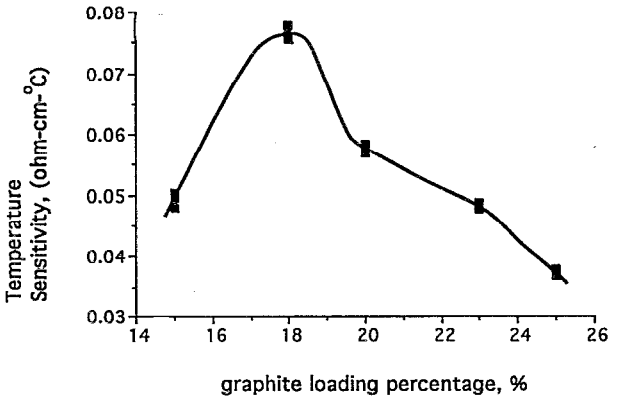

FIG. 11. Temperature sensitivity of the composite material as a function of the graphite loading percentage. Values were obtained at a relative humidity of 35%.

graphite loading. The slope of this line can be taken as a measurement of the sensitivity of the material to temperature. As expected, the sensitivity is a maximum at 18%, reaching a value of 10 Ω cm °C. A plot of temperature sensitivity versus loading percentage is given in Fig. 11. The similarity in shape between Figs. 9 and 11 suggest that the residual tensile stress due to the thermal expansion of the polyimide at high temperature is the major contributor to the temperature sensitivity. Low thermal expansion coefficient polyimides may exhibit this effect to a lesser degree.

CONCLUSION

A plasma processable, piezoresistive, graphite/polyimide thin film composite has been introduced for use in microsensor applications. A model has been presented for the determination of the mechanical and piezoresistive characteristics of thin films of this material under residual tensile stress. Using the model, graphite-filled polyimide thin films have been characterized for a range of 15–25 wt % graphite loading using load/deflection techniques. The results indicate that the residual stress is uneffected by variations in graphite loading, while the Young's modulus increases with increased loading. The piezoresistive coefficient has been found to be a maximum of 16.8 at 18% graphite loading. Both the mechanical and piezoresistive properties of this material indicate that it may be useful in the fabrication of micromachined structures.

ACKNOWLEDGMENTS

This work was supported by the International Society for Hybrid Microelectronics (ABF) and by the National Science Foundation under Grant No. ECS-9117074. The donation of the polyimides used in this work by E. I. Dupont Inc. are gratefully acknowledged as well as material and equipment donations provided by Kodak and MicroSwitch. Microfabrication was carried out in the facilities of the Georgia Institute of Technology Microelectronics Research Center.

[1] L. T. Taylor and A. K. St. Clair, in the Proceedings of the First Technical Conference on Polyimides, Ellenville, NY, Nov. 10–12, 1982, pp. 617–646 (unpublished).
[2] L. T. Taylor, Proceedings of the Second International Conference on Polyimides, NY, Nov. 5–7, 1985, pp. 428–437 (unpublished).
[3] J. D. Rancourt, R. K. Boggess, and L. T. Taylor, in Ref. 2, pp. 438–452.
[4] D. G. Madeleine and L. T. Taylor, in Ref. 2, pp. 453–462.
[5] R. K. Boggess and L. T. Taylor, in Ref. 2, pp. 463–470.
[6] D. M. Stoakley and A. K. St. Clair, in Ref. 2, pp. 471–479.
[7] M. Mehregany, R. T. Howe, and S. D. Senturia, J. Appl. Phys. **62**, 3579 (1987).
[8] L.-S. Fan, R. T. Howe, and R. S. Muller, *IEEE Micro Electromechanical Systems Workshop*, Salt Lake City, UT, February 20–22, 1989 (IEEE, New York, 1989), pp. 40, 41.
[9] H. Guckel, T. Randazzo, and D. W. Burns, J. Appl. Phys. **57**, 1671 (1985).
[10] K. Najafi and K. Suzuki, in Ref. 8, pp. 96, 97.
[11] L.-S. Fan, Y.-C. Tai, and R. S. Muller, IEEE Trans. Electron. Devices **ED-35**, 724 (1988).
[12] Y.-C. Tai and R. S. Muller, *IEEE Solid-State Sensor and Actuator Workshop*, Hilton Head Island, SC, June 6–9, 1988 (IEEE, New York, 1988), pp. 88–91.
[13] K. E. Petersen and C. R. Gaurnieri, J. Appl. Phys. **50**, 6761 (1979).
[14] R. T. Howe and R. S. Muller, J. Appl. Phys. **54**, 4674 (1983).
[15] R. T. Howe and R. S. Muller, Sensors Act. **4**, 447 (1983).
[16] M. G. Allen, M. Mehregany, R. T. Howe, and S. D. Senturia, Appl. Phys. Lett. **51**, 241 (1987).
[17] O. Tabata, K. Kawahata, S. Sugiyama, and I. Igarashi, Sensors Act. **20**, 135 (1989).
[18] Y. S. Bokov, Soviet Microelectron. **14**, 210 (1985).
[19] E. I. Bromley, J. N. Randall, D. C. Flanders, and R. W. Mountain, J. Vac. Sci. Technol. B **1**, 1364 (1983).
[20] L. D. Clark and D. F. Edell, *IEEE Micro Robots and Teleoperators Workshop*, Hyannis, MA, November 1987 (IEEE, New York, 1987), pp. 1–9.
[21] S. Timenshenko and K. Woinowsky-Krieger, *Theory of Plates and Shells* (McGraw–Hill, New York, 1940), Chap. 1.
[22] C. L. Bauer and R. J. Farris, Polymer Eng. Sci. **29**, 1107 (1989).
[23] F. Maseeh and S. D. Senturia, in the Proceedings of the Third International Conference on Polyimide, Ellenville, NY, November 2–4, 1988, pp. 575–584 (unpublished).
[24] H. Guckel, C. Rypstat, and M. Nesnidal, *IEEE Solid-State Sensor and Actuator Workshop*, Hilton Head, SC, June 22–25, 1992 (IEEE, New York, 1992), pp. 153–156.